General Disclaimer

One or more of the Following Statements may affect this Document

- This document has been reproduced from the best copy furnished by the organizational source. It is being released in the interest of making available as much information as possible.

- This document may contain data, which exceeds the sheet parameters. It was furnished in this condition by the organizational source and is the best copy available.

- This document may contain tone-on-tone or color graphs, charts and/or pictures, which have been reproduced in black and white.

- This document is paginated as submitted by the original source.

- Portions of this document are not fully legible due to the historical nature of some of the material. However, it is the best reproduction available from the original submission.

C S S A

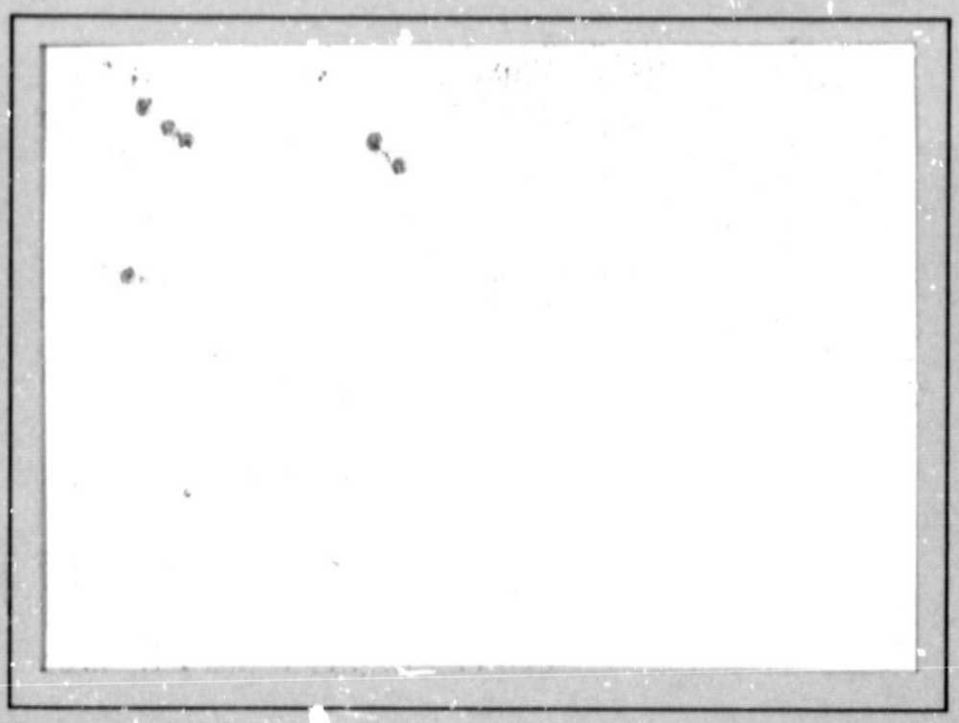

CENTER FOR SPACE SCIENCE AND ASTROPHYSICS
STANFORD UNIVERSITY
Stanford, California

EVOLUTION OF THE LUMINOSITY FUNCTION OF EXTRAGALACTIC OBJECTS

Vahé Petrosian
Center for Space Science and Astrophysics
Stanford University
Stanford, CA 94305

CSSA-ASTRO-85-18.
May 1985

Invited paper presented at the meeting on
STRUCTURE AND EVOLUTION OF ACTIVE GALACTIC NUCLEI
organized jointly by Tieste Astronomical Observatory and the
International School for Advanced Studies
Trieste, Italy

EVOLUTION OF THE LUMINOSITY FUNCTION OF EXTRAGALACTIC OBJECTS

Vahé Petrosian
Center for Space Science and Astrophysics
Stanford University
Stanford, CA 94305

ABSTRACT. A non-parametric procedure for determination of the evolution of the luminosity function of extragalactic objects and use of this for prediction of expected redshift and luminosity distribution of objects is described. The relation between this statistical evolution of the population and their physical evolution, such as the variation with cosmological epoch of their luminosity and formation rate is presented. This procedure when applied to a sample of optically selected quasars with redshifts less than two shows that the luminosity function evolves more strongly for higher luminosities, indicating a larger quasar activity at earlier epochs and a more rapid evolution of the objects during their higher luminosity phases. It is also shown that absence of many quasars at redshifts greater than three implies slowing down of this evolution in the conventional cosmological models, perhaps indicating that this is near the epoch of the birth of the quasar (and galaxies). However, it has been shown that the same is not true in all cosmological models, in some of which the epoch of birth could be at much higher redshifts.

I. INTRODUCTION

I will describe the steps and procedure required for determination of the evolution of the luminosity function of extragalactic objects and apply the results to quasars and, in particular, address the question of the evolution at redshifts higher than three. The purpose of such a study, of course, is to learn about the formation and evolution of the population. There are four distinct steps involved in this procedure. These are:

Selection of complete samples with known observational selection effects.
Choice of a cosmological model.

Statistical analysis of the sample and determination of the evolution of the luminosity function.
Use of the luminosity function for determination of the formation rate and the physical evolution of the objects.

These steps are described in the next section and are applied to a sample of quasars in Section III. A short summary is presented in Section IV.

II. THE PROCEDURE

A. The Selection of the Sample

Ideally, one requires a complete sample with known selection effects. The simplest case is obtained when the sample is limited by magnitude at one wavelength band. Then the data will consist of objects with known redshifts z and flux densities $f(\nu)$ greater than some limiting flux density f_o and can be represented by the following distribution function

$$n(f,z) = \sum_{i=1}^{N} \delta(f - f_i)\delta(z - z_i) \quad , \qquad (1)$$

where N is the total number of objects in the sample. Unfortunately, more than one criterion is needed for identification of the objects. If f above stands for some optical flux density, then the radio or X-ray flux densities of the object will determine their membership in a radio or X-ray sample, so that the distribution in general is multivariate rather than bivariate as in Equation (1). This aspect of the problem is not a source of difficulty but adds to the complexity of the calculations. We shall limit our discussion to optically selected samples. Even in this case, however, there are additional selection criteria like color in selections based on UV excess or line strength in selections based on slitless spectra. These put additional known limits on the sample such as $z < 2.2$ for UV excess samples or $z > 1.8$ for samples based on slitless spectra and perhaps some other unknown limit. We shall ignore the latter, which remains controversial, even though there has been considerable discussion about it in the past.

B. The Cosmological Models

The observed distribution [Eq. (1)] is not only a reflection of the luminosity function but also of the cosmological model. In general, the effects of the cosmological model cannot be separated from the evolution of the luminosity function. One needs to specify one of these two unknowns to determine the other. It is customary to assume a cosmological model and derive the luminosity function in that model. And it turns out that, because of the wide dispersion of the luminosity function and the small differences between the conventional cosmlogical

models at moderately low redshifts, $z < 2$, changing the cosmological model does not affect the outcome significantly. However, when dealing with the luminosity function at higher redshifts, in particular, for addressing the questions in regard to the turn-on redshift of the objects (quasars or galaxies), the differences in the cosmological models, especially if one is not limited to the conventional models with zero cosmological constant, becomes significant. Consequently, and because the new cosmological scenarios like the inflationary models suggest wider possibilities for the cosmological model, I shall consider three widely different cosmological models.

The first two models will be based on an inflation scenario that requires a negligible space curvature now and in the past since the epoch of inflation. This means that if we neglect the contribution of zero rest mass (or relativistic) particles, the cosmological constant Λ can be expressed in terms of the density parameter Ω (of non-relativistic matter) as $\lambda = \Lambda/3\ H_0^2 = 1 - \Omega$ (cf., e.g., Peebles 1984). Since $\Omega > 1$ or $\lambda < 0$ models can be ruled out because of their short ages (note that for $H_0 = 100$ km s^{-1} Mpc^{-1}, the $\Omega = 1$ model is already in difficulty), I shall consider two extreme models: $\Omega = 1.0$, $\lambda = 0$, and $\Omega = 0$, $\lambda = 1.0$. I shall also consider a third model that is not based on the inflationary scenario but is a closed-world model with negligible curvature now but in which the curvature was important in the near past giving rise to a quasistatic period of the expansion. For the parameters of this model I use $\lambda = 1.2$ and $\Omega = 0.1$. These three models are called the Einstein-deSitter, the deSitter, and the Lemaître models, respectively.

Given the cosmological model, we can then calculate for each object its intrinsic flux (or luminosity) at a specified rest frame frequency

$$F_i(\nu) = 4\pi D_L^2(z,\alpha,\Omega,\lambda)\ f_i(\nu) \quad , \tag{2}$$

and a new distribution (dropping the frequency dependence)

$$n(F,z) = \sum_{i=1}^{N} \delta(F - F_i)\delta(z - z_i) \quad , \tag{3}$$

where D_L is the luminosity distance and depends on the redshift, the cosmological parameters, and the spectral index $\alpha = -d\ln f(\nu)/d\ln \nu$. The variation of D_L with z (for $\alpha = 0.5$) is shown in Figure 1 for the above three models. Note that for the Lemaître model at a redshift $z \simeq 2$ one has reached the so-called antipode of the closed universe where $D_L \to 0$ and for a given luminosity F the flux density $f \to \infty$. However, such a drastic brightening of the sources near the antipode will be diminished by the presence of inhomogeneities in the distribution of matter (such as galaxies and clusters). The exact form of the D_L vs z curve then depends on the characteristics of these inhomogeneities. For a detailed discussion of this the reader is

referred to Petrosian and Salpeter (1968). The dashed line in Figure 1 is an example with some assumed size and distribution of the inhomogeneities. However, for simplification of the calculations, I will assume the solid line, which on the average will give a result similar to that of the more realistic dashed line. This will satisfy my purpose here, which is to show the extent of the differences between these widely different cosmological models.

C. The Luminosity Function

The bivariate luminosity function $\psi(F,z)$ can formally be related to the observed distribution by

$$\psi(F,z) = w(F_i,z_i)n(F,z) \quad , \tag{4}$$

where w is the weight of each object. These weights would be unity if there were no selection bias. However, because of the selection biases, objects of given F and z, which are less likely to be present in the sample, carry higher weights. The problem then is reduced to determination of the weights. The usual procedure, however, has been to parameterize the luminosity function and then find the value of the parameters bypassing the difficult but more accurate procedure of determining the weights. The use of the parameters determined in this manner for prediction of the expected number of objects outside the range of the parent sample (e.g., extension to deeper samples or higher redshifts) may give misleading results. The optimum procedure is to use a non-parametric procedure in the determination of the weights and as far as possible use these weights for further predictions.

The simplest non-parametric approach is to divide the area of the F-z plane accessible to the particular sample into various bins (as in Figure 2a) and from this find the ratio of the luminosity function at different bins. If the sample is large, the bins could be numerous and from the ratios of the numbers $n_{i,j}$ in different bins one can construct the differential luminosity function. In general, this is not the case, and the number of sources in the sample is small. It is more convenient to define the cumulative luminosity functions

$$\Phi(F,z) = \int_F^\infty \psi(F',z)dF' \quad , \quad \sigma(z,F) = \int_0^z \psi(F,z')dz' \quad , \tag{5}$$

which increase stepwise at values F and z of each source, respectively. The size of the steps are equal to the weights w. Graphic illustration of the cumulative functions is more convenient and more illuminating than the illustration of the delta fuction representation (Eq. (4)) of the differential luminosity function.

Referring to Figure 2a, we can then evaluate the ratios of the cumulative functions at different values of F and z. For example, consider the objects in the vertical strip between z_{i-1} and z_i and with $F > F_{min}(z_i)$, where $F_{min}(z)$ is the minimum value of F an object with

redshift z, must have in order to be included in the sample (i.e., to be below the heavy diagonal line). For these objects then

$$\frac{\Phi(F_j,z_i)}{\Phi(F_{j-1},z_i)} = 1 + \frac{n_{i,j}}{N_{i,j-1}} \quad , \qquad N_{i,j} = \sum_{r=o}^{j} n_{i,r} \quad . \tag{6}$$

It is clear that the repeated application of this equation at different F_j (starting from F_o) yields

$$\Phi(F_j,z_i) = \Phi(F_o,z_i) \prod_{r=1}^{j} \left(1 + \frac{n_{i,r}}{N_{i,r-1}}\right) , \qquad F_1 > F_j > F_{min}(z_i) \quad . \tag{7}$$

This procedure can then be repeated for all z_i as well as for horizontal strips at all F_j to obtain the $\sigma(z_i, F_j)$.

This method, however, ignores the few objects that may lie in the triangular regions bounded by the heavy lines of Figure 2a. As it will be shown more clearly below, in order to utilize all the information in the data fully, we can go to the limit of small bins so that each bin contains one object ($n_{i,j} \to 1$), in which case Equation (7) gives a result identical to that of Lynden-Bell's (1971) c^- method. Then we can extend this equation to objects in the triangular region if we define for them a new $N_{i,j}$. For example, for the object shown by the open circle, $N_{i,j}$ is equal to the number of objects in the shaded area. Clearly, an object in the triangular region carries more weight since the limit of the sample has excluded the object in the complementary triangle shown by the dashed lines. The fact that $N_{i,j}$ for this object may be smaller reflects this higher weight.

With this procedure we can then obtain two series of histograms $\Phi(F,z)$ and $\sigma(z,F)$, which can then be converted into the delta function form of the differential luminosity function or can be smoothed out and differentiated to yield $\psi(F,z)$. In general, because of the absence of low-luminosity objects at high redshifts and high-luminosity objects at low redshifts, the histograms $\Phi(F,z)$ at different z's [or $\sigma(z,F)$ at different F's] will have small overlapping regions. This makes it difficult to produce a complete description of the luminosity function throughout the accessible region of the F-z plane. Combining large sky area surveys with deeper but limited area surveys can alleviate this problem. In any case, without further assumptions about the luminosity function, we cannot extend it to the region outside the observed parts of the F-z plane for prediction of the expected distribution of sources in samples with different selection criteria. The above-mentioned histogram, however, may be helpful in choosing among various forms of the function $\psi(F,z)$.

The non-parametric procedure explained above becomes extremely useful if one can assume that the luminosity function is separable

$$\psi(F,z) = \psi(F)\rho(z) \quad , \tag{8}$$

which means that the two variables F and z are stochastically independent. In principle, a sizable sample can be used to determine the stochastic independence of the variables. In practice, however, this is difficult, and most procedures require some kind of binning of the objects. The alternate possibility is comparison of these data with numerically simulated data sets. The discussion of this is beyond the scope of this presentation, and I shall not dwell on it here. I will assume that, even if F an z are known to be stochastically dependent, there exist two other parameters, F_s and z_s, which are functions of F and z and are stochastically independent. In this case the data set can be transformed into these new variables and the analysis carried out in terms of them. For convenience I shall drop the subscript s from the discussion below and assume Equation (8), keeping in mind that F and z may no longer refer to the observed luminosity and redshift but may be arbitrary functions of them.

Given Equation (8), we can define new cumulative luminosity functions Φ and σ (see Eq. (5)) which are now functions of only one parameter. Note taht as defined here $\rho(z)$ is not the density per unit co-moving wolume V but is the marginal distribution in z. The density is equal to $\Phi(0)\rho(z)/(dV/dz)$.

$$\Phi(F) = \int_F^\infty \psi(F')dF' \quad , \qquad \sigma(z) = \int_o^z \rho(z')dz' \quad . \tag{9}$$

This also means that in Equation (6) both the numerator and the denominator can be integrated over the redshift from the minimum redshift of the sample to a maximum redshift $z_{max}(F_j)$, which yields

$$\frac{\Phi(F_j)}{\Phi(F_{j-1})} = 1 + \frac{n_j}{N_{j-1}} \quad , \qquad n_j = \sum_{k=o}^{i} n_{k,j} \quad , \qquad N_j = \sum_{k=o}^{i} N_{k,j} \quad , \tag{10}$$

where the bin i is determined by the luminosity F_i such that z_i is the maximum redshift that an object with luminosity F can have and still be in the sample. Now, in the limits of small bins, $F_j = F_{j-1} - dF$ and $\Phi(F_j) = \Phi(F_{j-1}) + \psi(F_j)dF$, Equation (10) can be written as

$$\frac{\psi(F)}{\Phi(F)} = -\frac{d\ln\Phi(F)}{dF} = \frac{n(F)}{N(F)} \quad , \tag{11}$$

where now

$$n(F') = \int_o^{z_{max}(F)} n(F',z')dz' , \qquad N(F) = \int_F^\infty n(F')dF' . \tag{12}$$

Similarly, we can write

$$\frac{\rho(z)}{\sigma(z)} = \frac{d\ln\sigma(z)}{dz} = \frac{m(z)}{M(z)} \quad , \tag{13}$$

with

$$m(z') = \int_{F_{min}(z)}^{\infty} n(F',z')dF' \quad , \qquad M(z) = \int_{o}^{z} m(z')dz' \quad . \tag{14}$$

The various quantities entering Equations (11) to (14), are illustrated in Figure 2b.

The data n(F,z) given by Equation (3) implies that n(F) or m(z) are just a series of delta functions at the luminosity or redshift of the objects in the sample and that N(F) and M(z) are histograms that increase by one every time an object is crossed (decreasing F or increasing z). Thus, Equations (11) and (13) can be written symbolically as

$$\frac{d\ln X}{dx} = \frac{\delta(x - x_i)}{N_i + \theta(x-x_i)} \quad , \tag{15}$$

where $\theta(x) = \int\delta(x)dx$ is the step function. Integration of (15) then yields

$$\delta\ln X_i = \ln\left(1 + \frac{1}{N_i}\right) \quad . \tag{16}$$

By this procedure we obtain two monotonically increasing histograms for the cumulative functions $\sigma(z)$ and $\Phi(F)$. Note that the quantity on the right hand side of equation (16) is well defined only if $N \to N_i$. As we start with the first object at lowest redshift (or highest luminosity), M (or N) will be zero. For sufficiently densely packed samples already, for the second object M could be equal to 1, and $\ln\sigma$ and $\delta\ln\sigma$ would be well defined. If not, we proceed to the first object with M or $N \neq 0$. If Φ_o and σ_o are the values of Φ and σ just below this object, then

$$\sigma(z_i) = \sigma_o \prod_{j=1}^{i}\left(1 + \frac{1}{M_j}\right) , \qquad \Phi(F_i) = \Phi_o \prod_{j=1}^{i}\left(1 + \frac{1}{N_j}\right) . \tag{17}$$

Once the cumulative functions are known, one may wish to smooth them out and differentiate to obtain the differential functions ψ and ρ. Or one may wish to keep the integrity of the data and express ψ and ρ in the delta function form of Equation (4). In Equations (11) and (13) if we replace the quantities n and m by this delta

function representation, we obtain

$$\rho(z) = \sum_i \frac{\sigma(z)}{M(z)} \delta(z - z_i) , \qquad \psi(F) = \sum_i \frac{\Phi(F)}{N(F)} \delta(F - F_i) , \quad (18)$$

which, when compared with Equation (4), means that the weights are

$$w(F_i, z_i) = \frac{\Phi(F_i)\sigma(z_i)}{N(F_i)M(z_i)} . \quad (19)$$

Note that F and z may not represent the real luminosity or redshift but some other parameters that are stochastically independent, in which case one can transform Equations (18) or (19) into the real luminosity and redshift domain.

Given these functions from the parent sample, we can make limited prediction about other samples. For example, for a sample with a different magnitude limit than that of the parent sample, the redshift or luminosity distributions, $m'(z)$ and $n'(F)$, can be obtained as follows:

$$m'(z)dz = \rho(z)dz\Phi\left(F'_{min}(z)\right) = \sigma(z)d\ln\,\sigma(z)\Phi\left(F'_{min}(z)\right) ,$$

$$n'(F)dF = \psi(F)dF\sigma\left(z'_{max}(F)\right) = -\Phi(F)d\ln\Phi(F)\sigma\left(z'_{min}(F)\right) , \quad (20)$$

where $F'_{min}(z)$ [or $z'_{max}(F)$] is the minimum (maximum) value of luminosity (redshift) that an object, with redshift z (luminosity F) must have in order to be in the new sample.

For z, F, $F_{min}(z)$ and $z_{max}(F)$ within the range of the parent sample histograms representing some integrals of m' and n' can be calculated without further assumptions or extrapolations. However, for extending such predictions to regions outside the observed domain of the parent sample, one needs further assumptions. For example, to determine the number of expected objects at redshifts larger than the highest so far observed in any complete sample, we need to extrapolate $\sigma(z)$ to higher z values. In the next section we shall need to carry out such extrapolations.

D. The Source Function and Physical Evolution

The aim of the investigation of the luminosity function and its statistical evaluation is to determine the physical evolution, F(t), of the objects with cosmic time and the source function S(F,t), which describes the rate of their formation as a function of cosmic time. The luminosity function can be expressed in terms of cosmic time $\psi(F,t) = \psi(F,z)dz/dt$ through the redshift-time relation of the specific

cosmological model. As mentioned above $\psi(F,t)$ stands for the total number of object (of luminosity F) within a specified co-moving volume and is related to F(t) and S(F,t) through the equation of continuity:

$$\partial\psi(F,t)/\partial t + \partial[\dot{F}\psi(F,t)]/\partial F = S(F,t) \quad , \qquad \dot{F} \equiv dF/dt \ . \quad (21)$$

Clearly this single equation is not sufficient to determine both S(F,t) and F(t) (or $\dot{F}$). We need further information or assumptions. Very little attention has been paid to this equation except recently by Cavaliere (see this proceedings) and his colleagues. They have assumed various forms for F(t) and S(F,t) and compared the derived $\psi(F,t)$ from the solution of Equation (21) with the observed luminosity function such as that derived by Schmidt and Green (1983). I think it will be more profitable to reverse this procedure in the sense of solving Equations (21) for S(F,t) (or $\dot{F}$) for a given ψ (F,t) and an assumed $\dot{F}$(or S(F,t)). As our discussion in the previous part shows, the analysis of the data yields directly the cumulative luminosity function rather than the differential function ψ (F,t). Therefore, if we integrate Equation (21) over F and t, we can express the cumulative source function in terms of the cumulative luminosity function. For the purpose of the illustration, let us consider the simple but plausible case where the luminosity function is separable, as in Equation (8), and $\dot{F}$ is independent of the cosmological epoch. Then, integrating Equation (21) over time and luminosity and noting that $\rho(t = 0) = 0$ and $\psi(F = \infty) = 0$, we obtain

$$\mathcal{S}(F,t) = \int_F^\infty dF' \int_0^t dt' S(F',t') = \rho(t)\Phi(F) + \dot{F}\sigma(t)\psi(F) \ . \quad (22)$$

Now, with the help of Equation (18), we can relate the cumulative source function $\mathcal{S}$ to the data directly as

$$\mathcal{S}(F,t) = \sum_i \sigma(z)\phi(F)\left[\frac{\delta(z-z_i)}{M(z)}\ \frac{dz}{dt} + \frac{\delta(F-F_i)}{N(F)}\ \frac{dF}{dt}\right] \ . \quad (23)$$

The use of such equations is beyond the scope of the present work. I am presenting these equations to indicate the complexity of the problem and to show how far we are from a direct determination of the source function S(F,t).

Luminosity or Number Evolution: There has been considerable discussion in the past and in this symposium in regard to whether the evolution of quasars and active galactic nuclei can be represented by a luminosity function that undergoes a pure density or a pure luminosity evolution. To begin with, I would like to point out that when referring to density one is talking about the number of objects in a unit co-moving volume, which is proportional not to the density of

objects at different epochs but to number of objects within a specified co-moving volume. (For a closed universe this could be the total number of objects). Consequently, number evolution is a more appropriate term than density evolution.

A thorough discussion of the possible evolutionary forms of the luminosity function was given in a paper by Lynds and Petrosian (1972). Most of the evolutionary forms discussed in this symposium, notably those by Schmidt, Weedman, and Koo, were fully covered in that earlier paper. Most importantly, however, what Roger Lynds and I stressed was the difference between what we called the statistical and the physical evolutions. The confusion between these remains the main source of controversy. What one normally calls the evolution of the luminosity function, which deals with the mathematical representation of the data by the function $\psi(F,z)$, is a statistical evolution of the population. The physical evolution of sources are described by the function $\dot{F}$ and the source function S in Equation (21).

I suggest that it is more appropriate to tailor the nomenclature to the physical processes rather than to the mathematical representation. To illustrate how this can be done, let me compare the time scales associated with the three terms in Equation (21). The first term has a time scale of the order of Hubble time τ_H ; $\partial\psi/\partial t \simeq \psi/\tau_H$. The second term is of the order of ψ/τ_F, where $\tau_F = F/\dot{F}$, and the time scale of the third term is determined by the time scale τ_S of the formation rate of the objects: $S(F,t) \simeq \psi/\tau_S$.

If $\tau_F \simeq \tau_H >> \tau_S$, which could be the case for $t > t_c$ if all the sources are created prior to an epoch t_c, then any evolution of ψ is a reflection of the physical luminosity evolution. The total number of objects (integrated over all luminosities) is a constant. Therefore, the term luminosity evolution is an appropriate term here. However, it should be stressed that this does not guarantee a pure luminosity evolution. The pure luminosity evolution requires that all sources, irrespective of their initial state or environment, evolve the same way, $F(t) = F_0 g(t)$.

In the other limiting case, where $\tau_S \simeq \tau_H >> \tau_F$, each source evolves very rapidly so that the luminosity function is determined primarily by the rate of formation of the sources. This may be called a number (or density) evolution. However, this again does not mean a pure density evolution model, which requires $S(F,t)$ to be a separable function of F and t.

III. EVOLUTION OF QUASARS

I will now use the procedure developed in the preceding section to determine the statistical evolution of the optical luminosity function of the quasars and, comment on the physical evolution of the sources. As discussed above, this procedure requires a knowledge of the appropriate stochastically independent parameters before one can determine the global evolution of the luminosity function over the wide ranges of the observed luminosity and redshift. Lacking this knowledge

I consider evolution over limited redshift and luminosity ranges, in which case I can assume that redshift and luminosity are stochastically independent. This assumption is a good approximation (and more readily testable) over small ranges of F and z.

The main new result I would like to concentrate on here is the question of cutoff of the luminosity function at high redshifts ($z > 3$). However, before doing this I will briefly describe the evolution of the luminosity function at low redshifts ($z < 2$), in which case the difference between the various cosmological models is insignificant as compared to the dispersion of the luminosity function.

A. Evolution at "low" redshifts ($z < 2$)

In one of the first analyses of a complete optically selected sample (Petrosian 1973), I had concluded that the distribution of the low luminosity, low redshift quasars can be described by a non-evolving luminosity function while a strong evolution was required for higher luminosity (higher redshift) objects. Now the new more extensive PG sample essentially confirms this earlier result (Schmidt and Green 1984), except that Schmidt and Green describe the distribution by a luminosity function whereby the evolution of the number of sources becomes monotonically stronger at higher and higher luminosities. In a short paper presented at the 1982 Liege conference (Petrosian and Jankevics 1982), it was shown that when the PG sample is divided into two (high and low luminosity) parts one finds that the low luminosity part shows no evolution while the high luminosity part shows strong evolution of number of quasars (cf. Figure 3). In the same paper it was also shown that the pure luminosity evolution with the parameters derived by Marshall et al (1983) does not agree with the PG sample. (A different set of pure luminosity evolution parameters can be found for a reasonable agreement; H. Marshall, private communication.) But there is no escaping of the fact that whatever the evolution of the luminosity function it is small or non-existant at low F but become significant at high values of F. Figure 3 clearly demonstrates this where, assuming a pure density evolution, it is shown that for low luminosities $\sigma(V) \propto V$ [i.e. $\rho(V)$ and $\rho(z)$ are constants] while for high luminosities $\sigma(V) \propto V^4$, implying a strong evolution.

This kind of behavior can be described by the following simple physical conditions. Suppose the rate of physical evolution of quasars is independent of the cosmological epoch t but depends on the luminosity F: e.g., $\dot{F} \propto F^{-\alpha}$. This is a reasonable assumption as it demands that quasars spend a shorter time in a higher luminosity state than in a lower one. For example, an equal energy consumption at different luminosity states implies $\alpha = 2$.

Let us first consider the luminosity function for high luminosities. At sufficiently high values of F (say $F > F_{cr}$), the lifetime $\tau_F = F/\dot{F}$ could be much shorter than the Hubble time τ_H so that on the right hand side of Equation (21) the first term is much smaller than the second and can be ignored. The rest of the equation can then be integrated to give

$$\psi(F,t) \propto F^{-\alpha} \int_F^\infty S(F',t)dF' \quad , \qquad F >> F_{cr} \quad , \tag{24}$$

which shows that a strong evolution (variation with t) is possible and that such an evolution is a reflection of the evolution of the creation rate of quasars. The observation that $\sigma(V) \propto V^4$ for high luminosity sources implies that $S(F,t)$ decreases rapidly as the universe expands. For values of $F << F_{cr}$, however, τ_F could become larger than the age of the universe so that now the second term in Equation (21) is negligible leading to the solution

$$\psi(F,t) = \int_o^t S(F,t')dt' \quad , \qquad F << F_{cr} \quad . \tag{25}$$

Because $S(F,t)$ was larger in the past (low t) and has decreased rapidly since then, it is obvious that for large values of t (low redshifts) the integral of S will be nearly independent of t explaining the observed absence of strong evolutions for weak sources.

Note that for $F << F_{cr}$ the luminosity function $\psi(F,t)$ is a reflection of the luminosity dependence of the source function (Eq. 25). But at high luminosities $\psi(F,t)$ is steeper than $S(F,t)$ by a power of $1 - \alpha$, indicating steepening of the luminosity function at high values of F because α is expected to be greater than unity. Such a steepening of the luminosity function is observed and can be used to determine the physical evolution of the quasars such as the luminosity dependence of the source function and the power law index α.

B. High redshifts and the redshift cutoff

One of the important cosmological questions has to do with the epoch of formation of galaxies and other structures. Theoretical arguments indicate that this epoch could correspond to a time anywhere from redshift 2 to 1,000. Because quasars are the only objects bright enough to be observed at such high redshifts, it is then expected that the evolution of their luminosity function at high redshift could shed light on this question.

There have been various attempts to extrapolate the evolution of the luminosity function to high redshifts and compare its consequences with observation, with the obvious conclusion that the strong evolution obtained from the data in the redshift ranges 1 to 2 cannot continue to very high redshifts. One of the most convincing results comes from Osmer's (1982) slitless spectroscopic search for quasars in the redshift range 3.7 to 4.7. This search yielded no quasars within this redshift range, prompting the conclusion that this may be the epoch of galaxy formation.

I would like to reconsider this problem, using the more rigorous method described in section II, for the three cosmological models mentioned there. As is shown in figure 1, the cosmological models begin to diverge from each other significantly (relative to the

dispersion in the data) only at large redshifts and are expected to give different results.

1) The Sample: The sample of sources I use are selected from the complete samples compiled by Schmidt and Green (1983) which, in addition to the PG sample, includes the Braccesi AB sample (Braccesi, Formiggini and Gandolfi 1970) four slitless spectroscopic samples (Hoag and Smith 1978; Lewis, McAlpine and Weedman 1979; Osmer and Smith 1980; Sramek and Weedman 1978) and the Kron and Chiu (1981) sample. To this I have added the few objects from the deeper Braccesi DF sample (Marshall et al 1983). In order to avoid extensive extrapolation over large cosmological distances and luminosities, I have limited the sample to the bright end of the luminosity which necessarily means limiting to high redshifts. The PG sample is sparse around redshift of 0.5 to 1.0 This turns out to be a convenient point of separating the sample into two sets, a high and a low luminosity set. For each cosmological model the lower cutoff of luminosity is chosen to correspond roughly to that of the same object in the PG sample which has a redshift of 0.944. This same luminosity cutoff is then used for all the other samples. Consequently, the selected sub-samples are somewhat different in the three cosmological models. There are about sixty objects in each case within the redshift range of 1 to 3. This implies a co-moving volume change of less than one order of magnitude and a luminosity range of slightly larger than one order of magnitude for the whole sample.

2) The procedure: I will assume stochastic independence betweeen luminosity F and redshift z, or co-moving volume V(z), which, in view of small ranges of the parameters just mentioned (and as we will show by simple binning) is a reasonable assumption. Then the application of the procedure described in sectin II-C is straightforward except that combining of samples with complicated selection criteria requires some modification of that procedure. All the samples have the same luminosity limit but different magnitude limits. This does not affect the procedure. But the fact that the slitless spectroscopy has a lower redshift cutoff at $z = 1.8$ complicates the procedure. It is not clear how rapidly the efficiency of discovering sources increases from a small value for $z < 1.8$ to a constant and significant value above this redshift and whether this efficiency is constant over the whole redshift range when Ly-α falls in the proper bandwidth of the plates. I will assume a zero efficiency outside this range and a constant efficiency throughout the range. The results presented below will, of course, be altered if this is not the case.

The lower redshift cutoff does not change the equations for the evaluation of the cumulative luminosity function $\Phi(F)$. However, Equation (15) for the number (or the co-moving density) evolution at $z > 1.8$ is altered as follows:

$$\frac{d\sigma}{\sigma - \sigma(z=1.8)} = \frac{\delta(z-z_i)}{M(z>1.8)}\, dz \quad , \tag{26}$$

so that

$$\sigma(z_i > 1.8) = \sigma(z = 1.8) + \prod_{j+1}^{i} \left(1 + \frac{1}{\tilde{M}_j}\right) , \qquad (27)$$

where $\tilde{M}$ now includes only objects with $z > 1.8$ and $F > F_{min}(z)$. This modification requires some interpolation of $\sigma(z)$ around $z = 1.8$ which I will not go into here.

3) The results: I will first present some of the histograms $\Phi(F)$ and $\sigma(z)$ and then extrapolate them to evaluate the expected numbers at high redshifts.

a) The cumulative luminosity function $\Phi(F)$ is shown in Figure (4) for all three models. The shapes of these luminosity functions are approximately the same (showing steepening at high luminosity) for all three models except that the luminosity scale is different. To somewhat justify the assumption of the stochastic independence of F and z the total sample was divided into three redshift bins with equal numbers in each bin and the luminosity function $\Phi(F)$ was evaluated for each bin. Figure (5) shows this result for the deSitter model ($k = 0$, $\Omega = 0.0$, $\lambda = 1.0$). The small number of objects in each sub-sample (about 20) makes a detailed comparison difficult, but rough similarities between the three histograms show that the assumption of the stochastic independence (over the small redshift and luminosity range) will not lead to large errors.

b) The cumulative number evolution functions $\sigma(z)$'s are shown in figure (6). Clearly the predictions of the three cosmological models are quite different. However, as evident, the three models show similar strong evolution in the range $1 < z < 2$ mentioned above but begin to diverge at higher redshifts. In particular, the Lemaître model ($\lambda = 1.21$, $k = +1$, $\Omega = 0.1$) shows a very slow increase of $\sigma(z)$ with redshift for $z > 2$ while the other two models show that the strong evolution continues to redshift of up to 3 and may even continue further on up to the highest redshift in the samples. The value of $\sigma(z)$ for $z > 3$ is uncertain (dashed histogram) because there are very few (about 4) objects in this range. Consequently, it is difficult to extrapolate this curve beyond $z = 3.5$. For the deSitter and the Einstein-deSitter models I show two possible extrapolations. One of these extrapolates by fitting a straight line (dashed) to the upper portion of the $\ln\sigma - \ln V$ curve obtaining $\sigma(V) \propto V^{\beta}$ with $\beta = 2.8$ and 3.7 for the two models, respectively. (Note that this is a slower evolution than $\sigma(V) \propto V^4$ found at lower redshift, perhaps indicating the slowing down of the evolution.) The second extrapolation assumes no evolution which means $\sigma(V) \propto V$ (dotted lines). For the Lemaître model the extrapolation seems to be fairly obvious ($\ln\sigma(z) \propto 0.37z$) as the curve in the $2 < z < 3$ range is well defined.

c) Predictions: As an example I have calculated the predicted cumulative redshift distribution for a sample limited to 19.5 blue magnitude (for definition of the magnitude see Schmidt and Green

1983). This is done using Equation (29) with $F_{min}(z)$ evaluated for 19.5 magnitude. The result is shown by the inset in figure (6a) where the predicted values (dashed and dotted lines) for the two extrapolations of $\sigma(z)$ beyond redshift $z = 3$ are compared with the observations (solid lines). The agreement at low redshifts is not surprising since the observed sample in this comparison was part of the parent sample used in deriving $\sigma(z)$ and $\Phi(F)$. The important feature here, however, is the deviation of the strong evolution case (dashed line) from observations at redshift $z > 3$. This shows that, in this model, the evolution is already slowing down at $z > 3$. Note that no other extrapolation, except that for $\sigma(z)$, was needed for this calculation.

Further comparison between the prediction in the three cosmological models and observations are shown in Table I. For the first two models in this table there are two predictions based on the two extrapolations shown in figures 6a and 6b. The prediction at 19.5 limiting blue magnitude is compared with the data tabulated by Schmidt and Green (1983) (their table III, HS and SW List) taken from Hoag and Smith (1977) and Sramek and Weedman (1978). The first line on Table I shows that when the redshift range is divided into two parts each containing about the same number of objects (9 in one and 10 in the other in this case) the predictions agree quite well with the observation. However, if we compare numbers expected above and below redshift 3, we find that the first two models agree with observation if the sources do not evolve beyond redshift 3($\sigma(V) \propto V$). However, the third model gives acceptable results for the natural extrapolation shown in figure 6c.

The obvious conclusion from this is that in Lemaître type models the source evolution is found to have slowed down beyond $z > 2$ and could continue at this rate to a redshift of 3.5 while in the other two (inflationary) models the evolution must slow down and stop beyond redshift 3. This latter, however, is not a firm result because selection effects can account for absence of observed objects beyond redshift 3. An indication of this is shown on the third line of Table I where I compare the predicted and observed ratios of the number of high and low luminosity objects in the same sample. Because the luminosities of objects are different in the three cosmological models, the luminosity dividing the two bins will also be different. The latter is selected such that the observed ratio of the number of the objects in the two bins is about unity. As is evident too few low luminosity objects are observed as compared to the predictions of the two models. This could be caused by a bias against discovery of high luminosity objects by slitless spectroscopy. The so-called Baldwin effect (cf. e.g. Wampler et al 1984) can cause such a bias as the line equivalent width is smaller at higher luminosities making the discovery of such objects more difficult.

The strongest evidence for the decrease of the numbers at high redshifts is provided by Osmer's (1982) observations where the claim is that it goes deeper by 1.2 magnitude than the earlier Hoag and Smith (1971) observation (with a limiting magnitude of 19.5) and was designed to discover quasars in the redshift range $3.7 > z > 4.7$. None was

discovered in a search limited to a 5.1 sq. deg. area. Using the derived luminosity function and the extrapolations of $\sigma(z)$ mentioned above, I have estimated the expected numbers in this redshift range for a limiting blue magnitude of 20.7 for the three cosmological models. The predicted numbers are based on the observed numbers (at 19.5 magnitude) given in the parenthesis.

This, in agreement with Osmer's (1982) conclusion, clearly rules out the conventional Einstein-deSitter model with a strong evolution and, to a lesser degree, no evolution in this model and the strong evolution in the deSitter model. The deSitter model with no evolution beyond $z = 3$ and the Lemaitre model are acceptable considering the many uncertainties in the limiting magnitude, the completeness and possible selection bias of the samples.

IV. SUMMARY AND DISCUSSIONS

The study of statistical evolution of the luminosity function of extragalactic objects is important for understanding of the physical evolution of the objects and provides important clues about the variation with time of the birth rate and the luminosity of the objects and, in general, about the formation of structures in the universe. I have explained the necessary steps for a complete description of this evolution.

The first and the most difficult step in this study is an accurate statistical analysis of the distribution of objects in the redshift and luminosity domain once a sample and a cosmological model are selected. Parametric approaches suffer from the fact that they are not unique and that could lead to misleading results if extrapolated beyond the observed range of the variables. The non-parametric procedure described here works for a luminosity function which is separable into functions of some variables which need not be the basic variable, namely, the luminosity and redshift. Discovery of such stochastically independent variables is the difficult step which I have avoided here by considering the data for small ranges of the basic variables, in which case the assumption that these variables are stochastically independent is a good approximation.

Using results from earlier works, I have argued that at lower redshifts (mean redshift of about one) and independent of the cosmological model the luminosity function shows stronger evolution at higher luminosities than at lower luminosities. One interpretation of these results is that the activity in galaxies which leads to the quasar phenomenon was much more prevalent in the past and that the rate of the physical evolution of the luminosity of the quasars is a strong function of the luminosity in the sense that much shorter time is spent at a high luminosity phase than a low one.

The next question I have addressed here is how far into the past this ever increasing activity can be extrapolated and whether the existing data tells us about the cosmological epoch when this activity started. Here I have shown that the conclusion depends strongly on the cosmological model and that in conventinal cosmological models at

redshifts greater than three the activity must have been occurring at a much slower rate than the simple extrapolation would indicate, but that there are cosmological models where the activity could have been present at larger redshifts. Therefore, the epoch of the formation of quasars (and galaxies) remains an unknown.

ACKNOWLEDGMENT

I would like to thank Professor Paul Switzer of the Department of Statistics at Stanford University for helpful discussions on the statistical matters and acknowledge partial support from the National Aeronautics and Space Administration under Grant NGR 05-020-668.

REFERENCES

Braccesi, A., Formiggini, L. and Gandolfi, E. 1970, Astron. and Astrophys. 5, 264.

Hoag, A.A. and Smith, M.G. 1971, Ap. J. 217, 362.

Kron, R.G. and Chiu, L.-T.G. 1981, Publ. A.S.P. 93, 397.

Lewis, D.W., MacAlpine, G.M. and Weedman, D.W. 1971, Ap. J. 233, 787.

Lynden-Bell, D. 1971, Mon. Not. R. Astr. Soc. 155, 95.

Lynds, R. and Petrosian, V. 1972, Ap. J. 175, 591.

Marshall, H.L., Tananbaum, H., Zamorini, G., Huchra, J.P., Braccesi, A. and Zitelli, V. 1983, Ap. J. 269, 42.

Osmer, P.S. 1982, Ap. J. 253,28.

Osmer, P.S. and Smith, M.G. 1980, Ap. J. Suppl. 42. 333.

Peebles, P.J.E. 1984, Ap. J. 284, 439.

Petrosian, V. 1973, Ap. J. 183, 359.

Petrosian, V. and Jankevics, A. 1983, Quasars and Gravitational Lenses, Proc. of the 24th Liege Int'l. Astrophys. Colloq., Ed. J.P. Swings, pp. 250-257.

Petrosian, V. and Salpeter, E.E. 1968, Ap. J. 151, 411.

Schmidt, M. and Green, R.F. 1983, Ap. J. 269, 352.

Sramek, R.A. and Weedman, D.W. 1978, Ap. J. 221, 468.

Wampler, E.J., Gaskell, C.M., Burke, W.L. and Baldwin, J.A. 1984, Ap. J. 276, 403.

TABLE I

Comparison of the Observed and Predicted Number of Objects in the Three Cosmological Models

Model	k = 0* Ω = 1.0, λ = 0.0	k = 0* Ω = 0.0, λ = 1.0	k = +1 Ω = 0.1, λ = 1.21	Observed
a) 19.5 mag.				
$\frac{N(2.2<z<3.5)}{N(1.8<z<2.2)}$	0.71 1.5	1.3 2.0	1.2	9/10
$\frac{N(3<z<3.5)}{N(1.8<z<3)}$	1.8/18 7.4/18	1.1/18 6.7/18	2.2/18	1/18
$\frac{N(\text{High F})}{N(\text{Low F})}$	2.1	3.0	1.2	10/9
b) 20.7 mag.**				
N(3.7<z<4.7)	5.4 (10) 46	0.53 (2) 4.7	1.8 (9)	0

*First ratios from extrapolation assuming no evolution ($\sigma \propto V$); the second ratios from the evolutionary extrapolation (dashed lines Figure 6a, 6b).

**The calculated numbers are based on the number (shown in the parenthesis) of objects in the 19.5 magnitude limited sample.

FIGURE CAPTIONS

Figure 1. Luminosity distance $D_L(z)$ versus redshift for three cosmological models. For the $k = +1$, $\Omega = 0.1$, $\lambda = 1.21$ model the dashed line is a more realistic relation, but for simplification of calculations I have assumed the solid line. Spectral index α is assumed to be 0.5.

Figure 2. Schematic representation of the distribution of object in the luminosity (F) - redshift (z) plane. The heavy solid line is the F-z relation at the limiting apparent flux value f_0. For each F (or z) this line defines the maximum z (or minimum F) that an object with this F (or z) can have and be in the sample.

(a) Defines the parameters when the analysis is carried out by binning the sample. $n_{i,j}$ is the number of objects in the bin with $F_j < F < F_{j-1}$ and $z_{i-1} < z < z_i$.

(b) Defines the parameter $z_{max}(F)$, $F_{min}(z)$ and M(z) and N(F) used in the text.

Figure 3. The cumulative density evolution function σ versus volume V (up to redshift z) for "low" redshift quasars ($z < 2$, PG sample, Schmidt and Green 1983) at high and low luminosities separately. Note for constant number (or co-moving density) $\sigma(V) \propto V$. The cosmological model assumed here is $\Omega = 0$, $\lambda = 0$, $k = -1$ but this result is not sensitive to the model. V_0 and V_0' are arbitrary volumes.

Figure 4. The cumulative luminosity function versus the blue absolute magnitude as defined by Schmidt and Green (1983) for the three cosmological models depicted on Figure 1. For clarity, the histograms are shifted to the right by the specified amounts. The relative values of $\Phi(M)$ are arbitrary.

Figure 5. The luminosity function for the $k = 0$, $\Omega = 0.0$, $\lambda = 1.0$ cosmological model for objects in three non-overlapping redshift ranges. For clarity two of the histograms are shifted up or down by the quantity X indicated. The rough similarity of these histograms shows that the assumption of stochastic independence of the luminosity (or absolute magnitude M_B) and redshift over the small ranges of these parameters will not lead to erroneous results.

Figure 6. The cumulative number (or co-moving density) evolution function $\sigma(z)$ versus redshift z, or volume V(z) up to redshift z, for the three cosmological models. The dashed portions of the histogram have larger uncertainties.

(a) $k = 0$, $\Omega = 1.0$, $\lambda = 0.0$.
(b) $k = 0$, $\Omega = 0.0$, $\lambda = 1.0$.
(c) $k = 1$, $\Omega = 0.1$, $\lambda = 1.21$.

In Figures (a) and (b) two possible extrapolations for $z > 3$ have been shown with one of them assuming no number or density evolution, $\sigma(V) \propto V$. The inset in (b) shows the predicted cumulative number of sources between $z_{min} = 1.8$ and z expected at blue limiting magnitude of 19.5 and for the two extrapolations shown in the main part. In (c) the steps of the histogram at $z > 2$ are smaller than the width of the line.

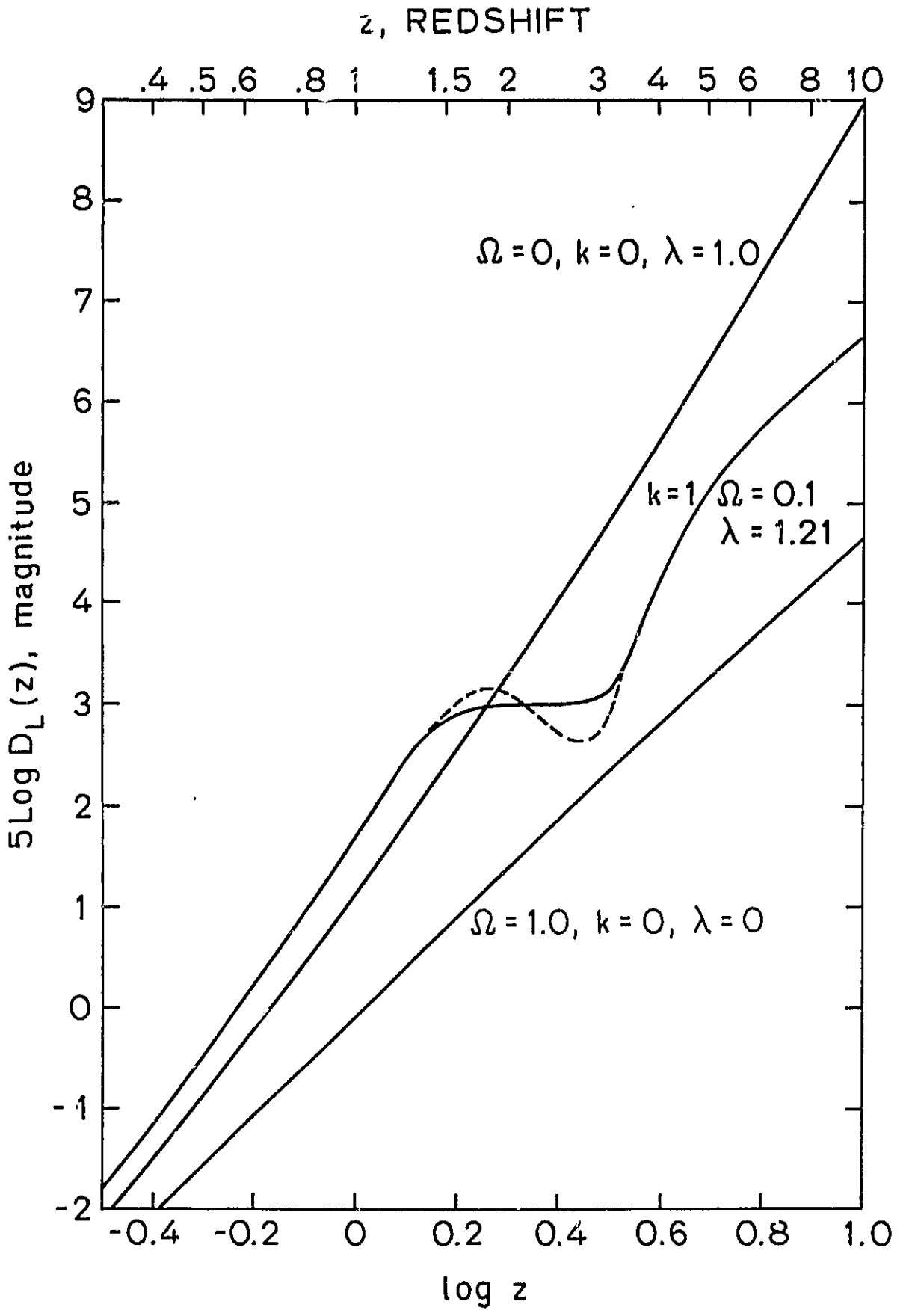
z, REDSHIFT
.4 .5 .6 .8 1 1.5 2 3 4 5 6 8 10
9
8
7
6
5
4
3
2
1
0
-1
-2
5Log D_L (z), magnitude
Ω = 0, k = 0, λ = 1.0
k = 1 Ω = 0.1
λ = 1.21
Ω = 1.0, k = 0, λ = 0
-0.4 -0.2 0 0.2 0.4 0.6 0.8 1.0
log z

Figure 1

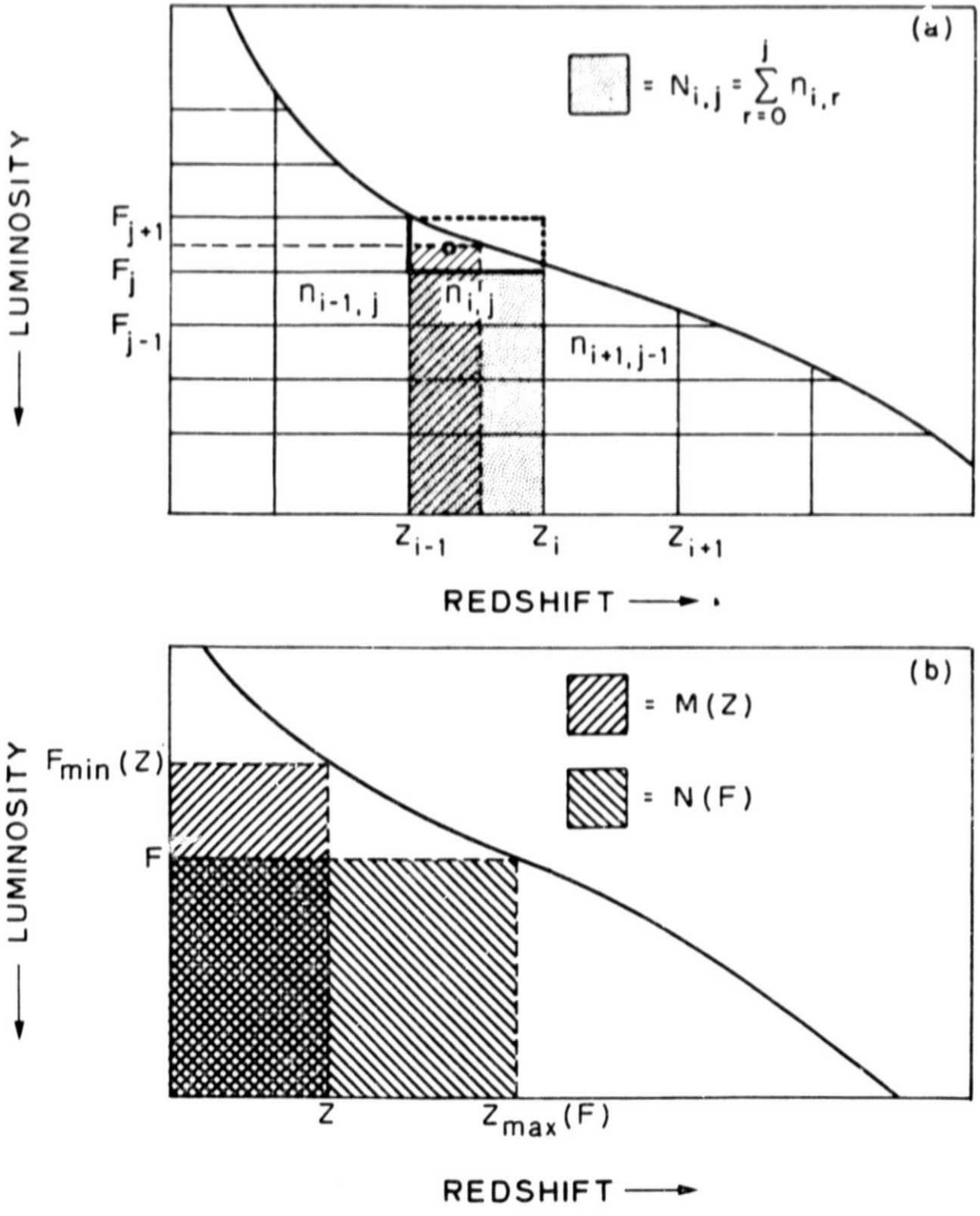

Figure 2

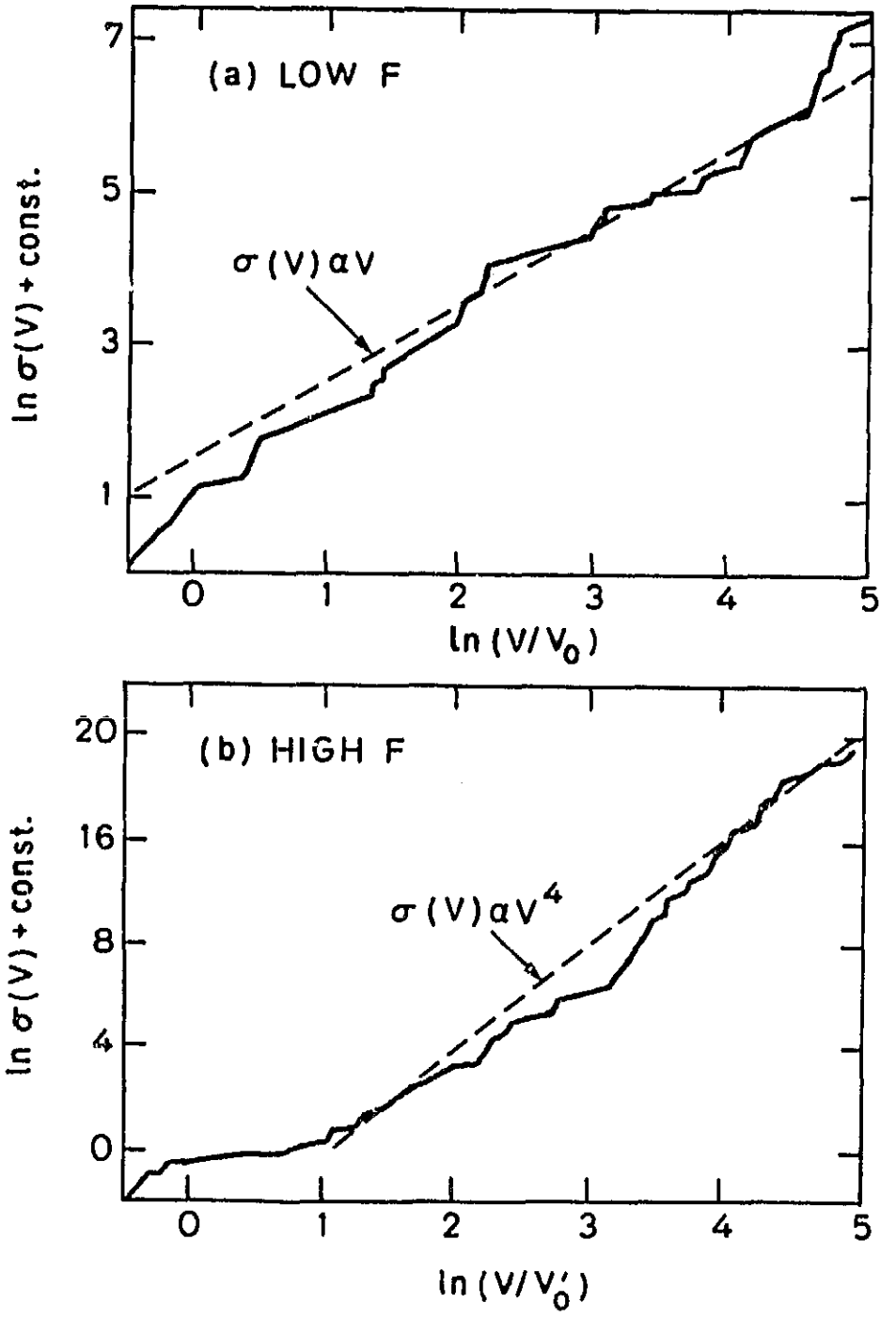

Figure 3

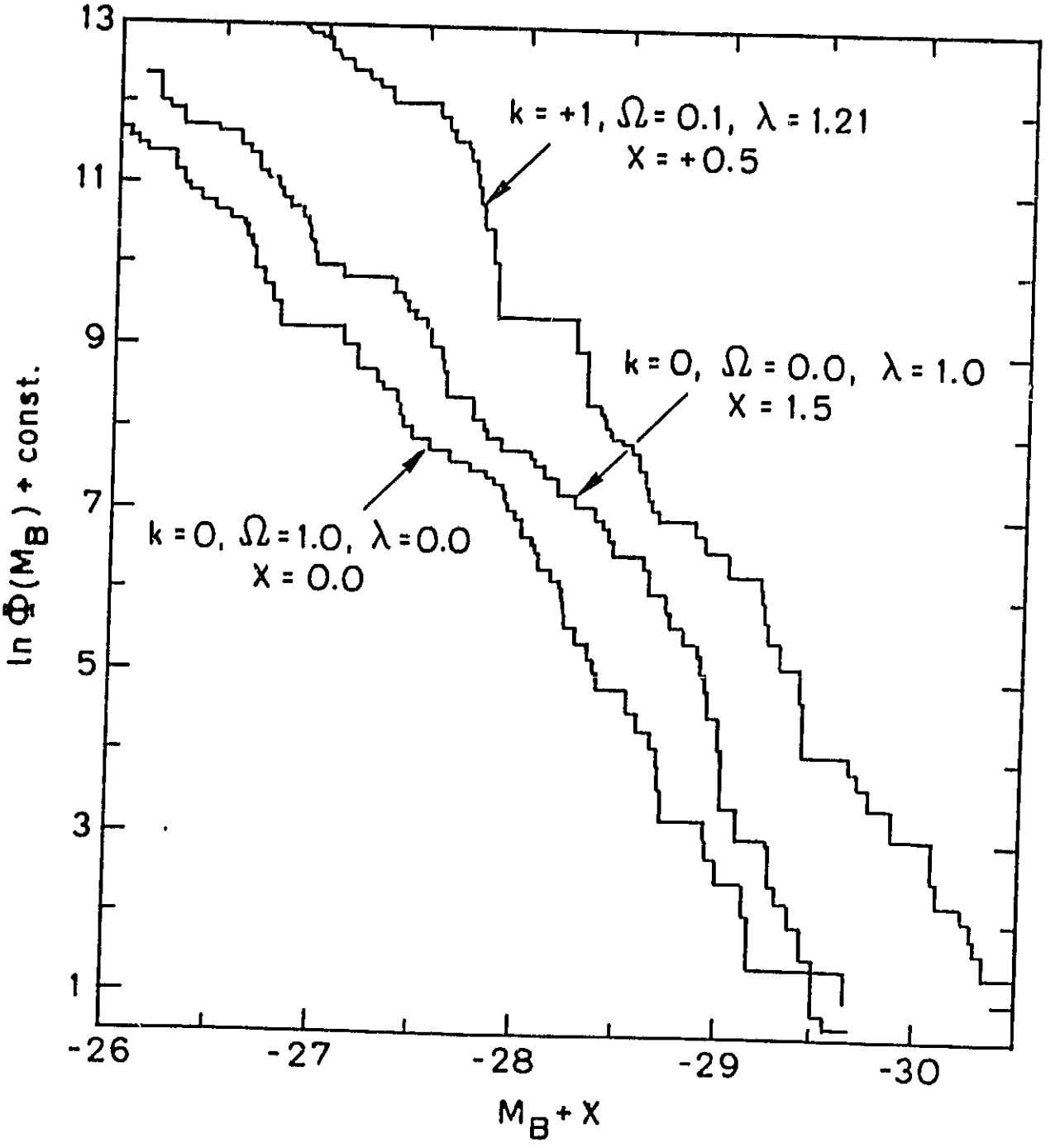
13
11
9
7
5
3
1
-26
-27
-28
-29
-30
ln Φ(M_B) + const.
M_B + X
k = +1, Ω = 0.1, λ = 1.21
X = +0.5
k = 0, Ω = 0.0, λ = 1.0
X = 1.5
k = 0, Ω = 1.0, λ = 0.0
X = 0.0

Figure 4

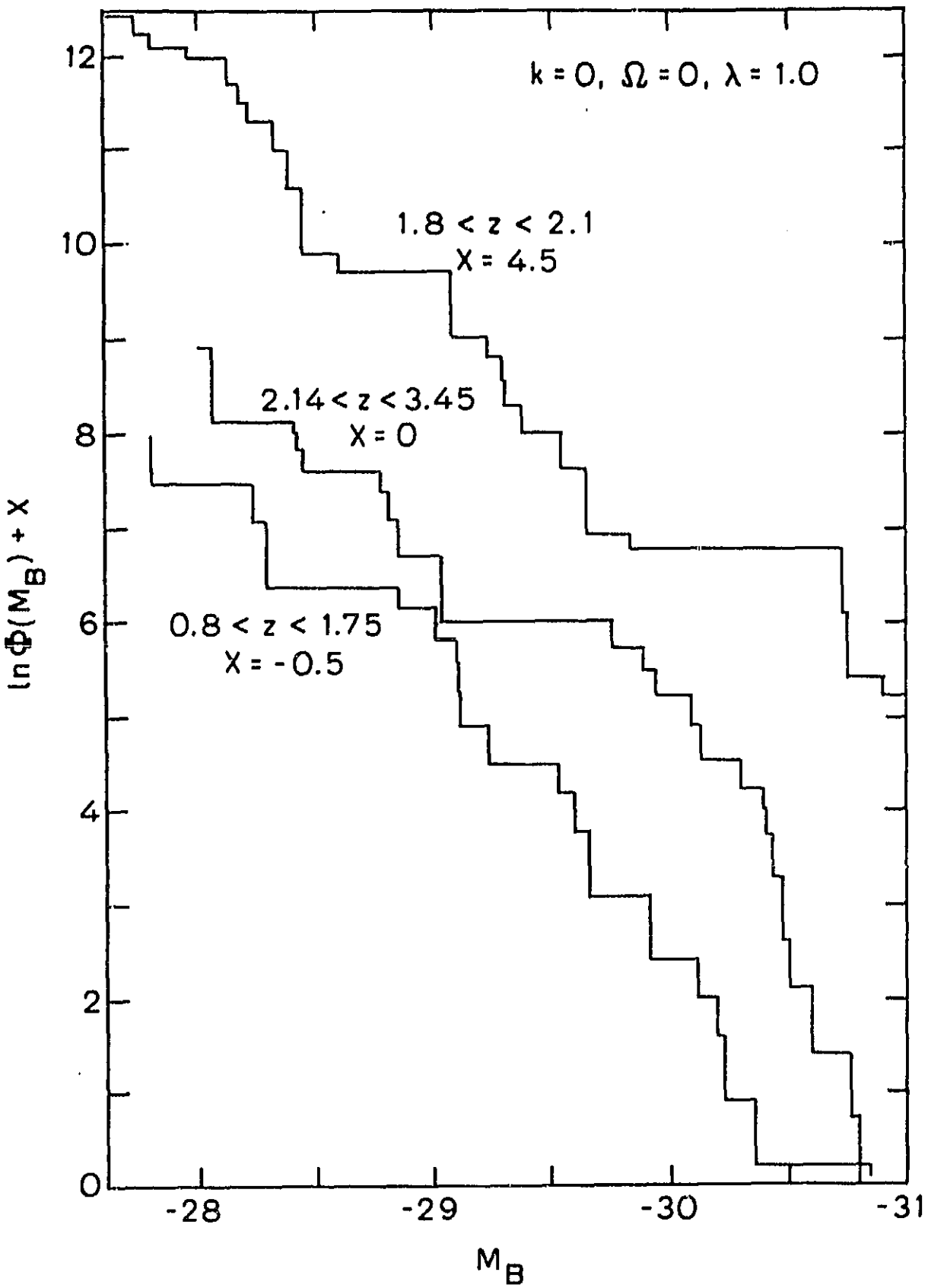
k = 0, Ω = 0, λ = 1.0
1.8 < z < 2.1
X = 4.5
2.14 < z < 3.45
X = 0
0.8 < z < 1.75
X = -0.5
ln Φ(M_B) + X
M_B
12
10
8
6
4
2
0
-28
-29
-30
-31

Figure 5

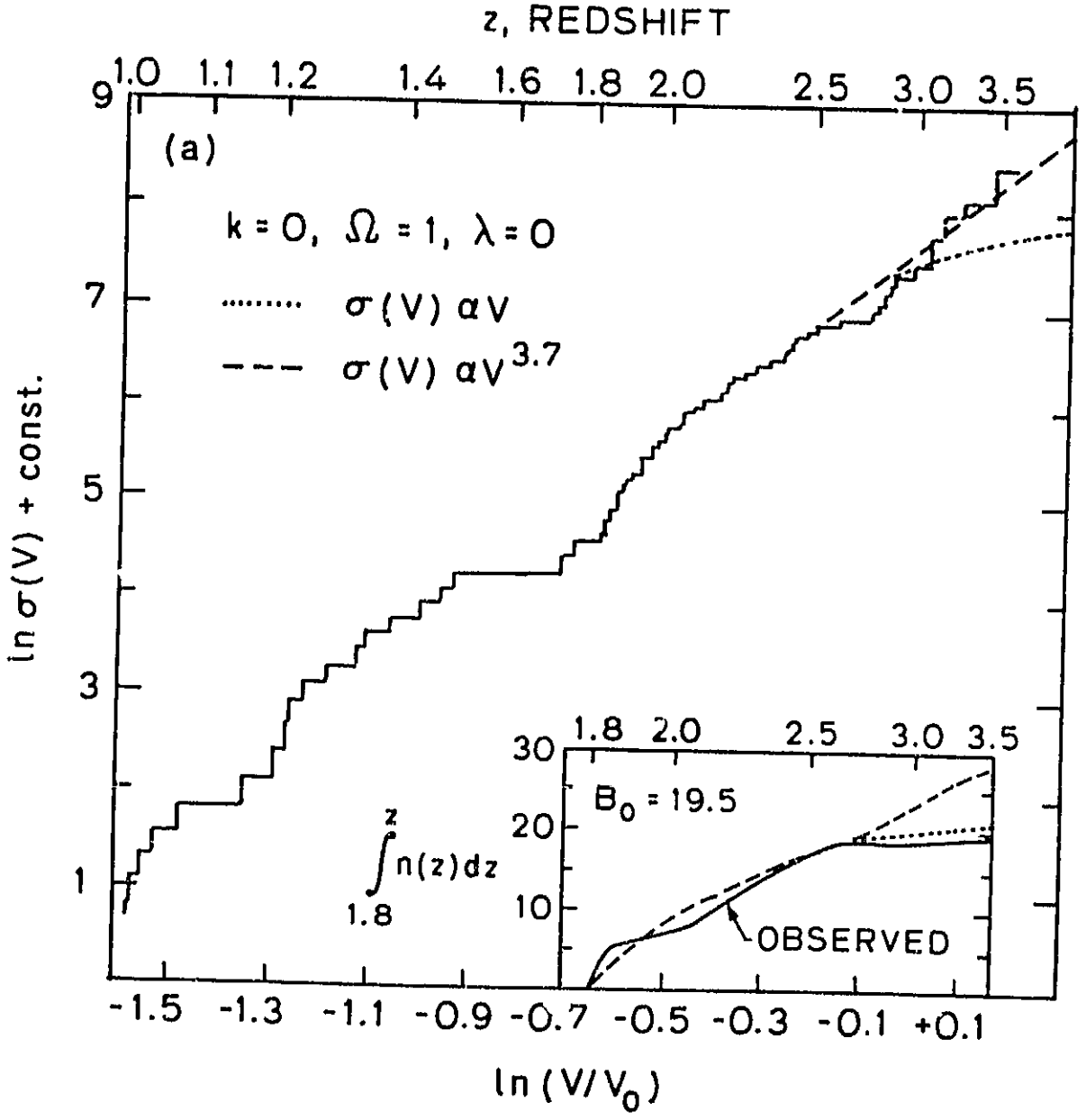
z, REDSHIFT
1.0 1.1 1.2 1.4 1.6 1.8 2.0 2.5 3.0 3.5
(a)
k = 0, Ω = 1, λ = 0
σ(V) αV
σ(V) αV^3.7
ln σ(V) + const.
9
7
5
3
1
1.8 2.0 2.5 3.0 3.5
30
20
10
B0 = 19.5
OBSERVED
∫ n(z)dz
1.8
z
-1.5 -1.3 -1.1 -0.9 -0.7 -0.5 -0.3 -0.1 +0.1
ln (V/V0)

Figure 6a

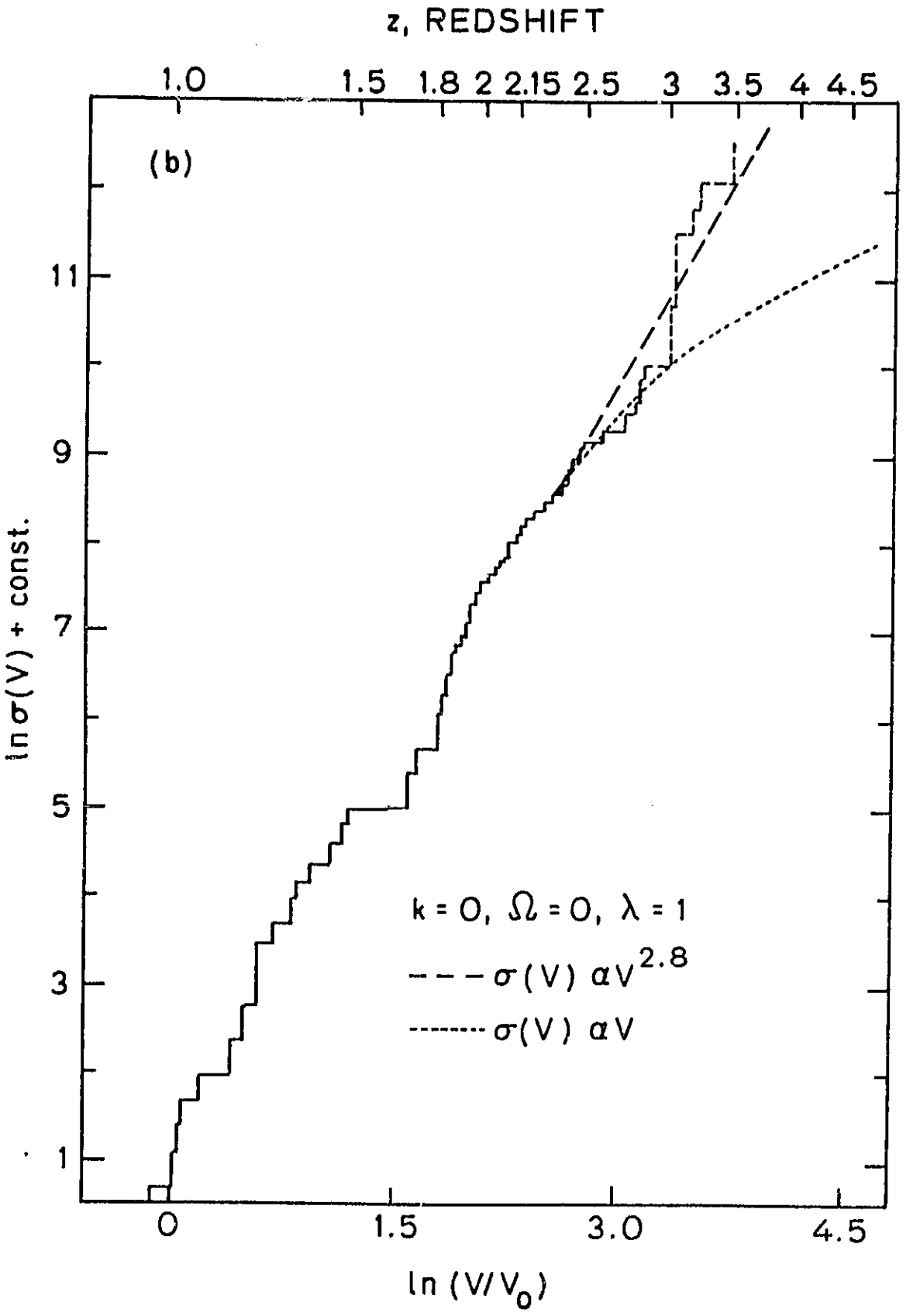
z, REDSHIFT
1.0
1.5
1.8
2
2.15
2.5
3
3.5
4
4.5
(b)
11
9
7
5
3
1
ln σ(V) + const.
k = 0, Ω = 0, λ = 1
– – – σ(V) αV^2.8
------ σ(V) αV
0
1.5
3.0
4.5
ln (V/V0)

Figure 6b

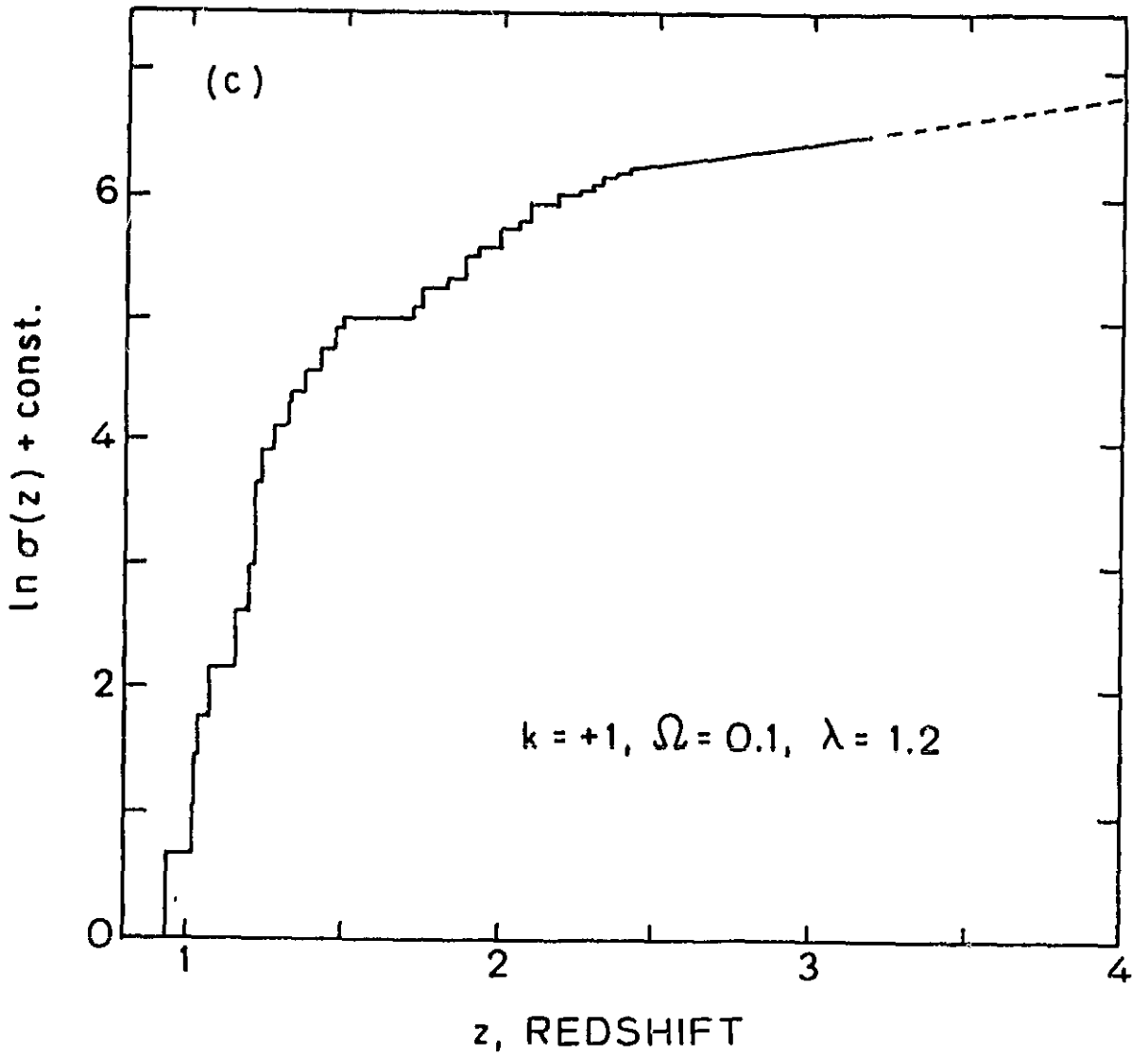

Figure 6c